THE PENNSYLVANIA STATE UNIVERSITY
SCHREYER HONORS COLLEGE

DEPARTMENT OF ENGINEERING SCIENCE AND MECHANICS

AN INVESTIGATION OF RESISTIVE RANDOM ACCESS MEMORY

WILLIAM R BARKER
SPRING 2019

A thesis
submitted in partial fulfillment
of the requirements
for a baccalaureate degree in
Engineering Science
with honors in Engineering Science

Reviewed and approved* by the following:

Patrick Lenahan, PhD
Distinguished Professor of Engineering Science and Mechanics
Thesis Supervisor

Corina Drapaca, PhD
Associate Professor of Engineering Science and Mechanics
Honors Adviser

*Signatures are on file in the Schreyer Honors College.

Abstract

This study evaluates two electron resonance spectroscopy techniques on an emerging memory technology, resistive random access memory. The first is electrically detected magnetic resonance, which is a well established spectroscopic technique used to investigate nanoelectronics. The second technique is near-zero field magnetoresistance, which is a new tool with the potential to provide information and functionally that electrically detected magnetic resonance cannot currently provide. 10 nm tantalum oxide resistive random access memory in a partially formed state was swept across 80 G centered at 0 G and with a 5 G modulation field. This analysis revealed a broad, asymmetric zero-field response, but no resonance response was present above the noise in the system. This study provides a preliminary spectroscopic analysis of resistive random access memory and is the first reported use of near-zero field magnetoresistance spectroscopy on a resistive random access memory device. While it does not provide any substantial evidence to support claims about the controversial formation and switching mechanisms discussed in current literature on resistive random access memory, this study provides clear evidence that further development of near-zero field magnetoresistance spectroscopy will be useful for the investigation of devices that are currently difficult to study with previously established electron resonance spectroscopy techniques.

Table of Contents

List of Figures

Acknowledgements

I would like to thank the researchers at Sandia National Laboratory, in particular David Hughart, for their technical input and for supplying me with ReRAM devices. Additionally, I would like to thank the graduate students of Penn State's Semiconductor Spectroscopy laboratory for their technical input and constant support throughout the entirety of this project.

Chapter 1

Introduction

1.1 Recording Information

For centuries, humans have found a means of recording information. Ancient people drew on the walls of caves; granaries recorded stock and religion on papyrus in the fertile crescent. Stone tablets were replaced by scrolls, and then by books. Handwritten notes were replaced by printing in the renaissance. Today, we find ourselves in a digital age, with knowledge recorded in ones and zeroes in discs and flash drives.

We know increasingly more of the past as inventors developed more effective means of recording information. Surely, much of what we do today will be read, rewritten, and reported by historians of the future. Much of this will be with greater clarity than is achievable by historians today, in part because of the advanced we have made in science and engineering. More practically, people today need effective means of recording information. Faster, more reliable memory and storage devices are needed to meet the future needs of computer users and consumers. Resistive

random access memory, or ReRAM, is a viable candidate for future memory and storage uses. Investigating the nature of these devices is pertinent for developing the next generation of recording tools.

1.2 Understanding Devices

The investigation of both ReRAM and other devices requires powerful analytical techniques. As scientists and engineers, it is increasingly important that new tools be developed and studied so that we may have a greater means of processing and studying devices. Researchers have, for some time, used resonance spectroscopy as a means of studying bulk materials. Later, these spectroscopic techniques were developed for use on electronic devices. Developing these techniques further is essential for aiding the study and production of the electronics used in tomorrow's computers, phones, and devices.

1.3 Overview

This study will outline the basics of electron spin resonance, as well as provide an introduction to the structure and operation of ReRAM. After, it will detail the methods used to develop both the aforementioned spectroscopic techniques and the understanding of ReRAM. These results will be presented and discussed, and future work for both resonance spectroscopy and ReRAM will be broadly outlined.

Chapter 2

Semiconductor Spectroscopy

2.1 Electron Paramagnetic Resonance

Electron paramagnetic resonance (EPR) is a technique which may be used to find paramagnetic species in a variety of materials [1]. Electrons have, as elementary particles, a quantized angular momentum that is referred to as the electron spin [2]. The quantization of this spin means that an electron has, at least one on confined direction, with a spin number of $\pm\frac{1}{2}$. While an electron in free space can move freely between both spin states, given that both spin states are at the same energy, an electron under a magnetic field cannot transition freely between both states. An electron under a magnetic field experiences a phenomena known as Zeeman splitting, depicted in figure 2.1 [2, 3]. The Zeeman splitting energy difference may be described via

$$\Delta E = g\mu_\beta BS \tag{2.1}$$

where ΔE is the energy difference between levels, g is the Landé factor (approximately 2.00232), μ_β is the Bohr magneton, or $\frac{-|e|h}{4\pi m_e}$, where m_e is the mass of the electron [2, 4].

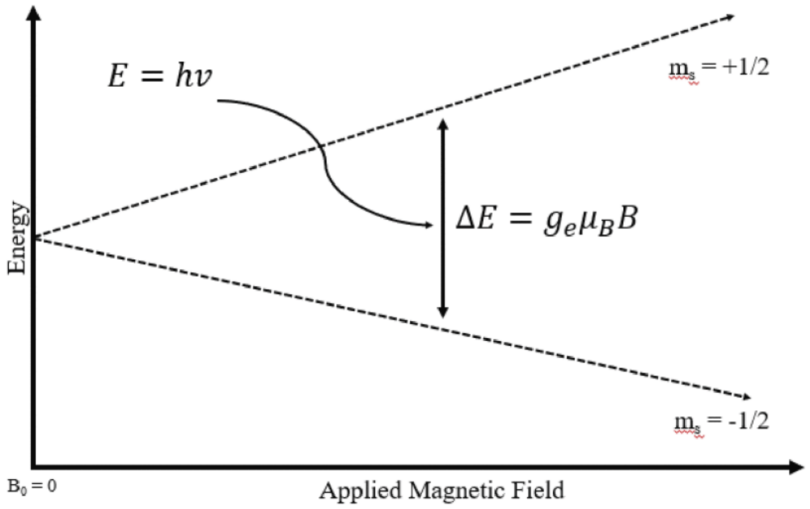

Figure 2.1: Illustration of Zeeman splitting. Figure from J. P. Ashton, S. J. Moxim, P. M. Lenahan, C. G. Mckay, R. J. Waskiewicz, K. J. Myers, M. E. Flatte, N. J. Harmon, and C. D. Young, "A new analytical tool for the study of radiation effects in 3-d integrated circuits: Near-zero field magnetoresistance spectroscopy," IEEE Transactions on Nuclear Science, vol. 66, no. 1, pp. 428–436, 2019.

Additionally, magnetic nuclei have a spin quantization component. Nuclei spin experience energy similar to that of electrons. This nuclear Zeeman effect is described via

$$\Delta E = g_N \mu_N B I \tag{2.2}$$

where all quantities are analogous to that in equation 2.1 except for I, which is the nuclear spin number [2]. The electron and nuclear interactions are called nuclear hyperfine interactions. These hyperfine interactions can affect the resonance condition of an electron in EPR. If an electron is interacting with many magnetic nuclei, then the energy level difference may be described via

$$E = g\mu_\beta BS + \sum \alpha_i I_i S \tag{2.3}$$

in which α is a hyperfine coupling constant, and i indicates each nucleus interacting with an elec-

tron [2].

In EPR, a resonant condition is found by applying a stable field of microwave frequency photons. Recall the expression for the energy of a photon,

$$E = h\nu, \tag{2.4}$$

where E is energy, h is the Planck constant, and ν is the frequency of the photon [2, 5]. Setting equal the photon energy to energy level difference from Zeeman splitting described by equations 2.4 and 2.1,

$$h\nu = g\mu_\beta B. \tag{2.5}$$

This relationship is the fundamental basis for practical EPR spectroscopy [6, 4].

Equation 2.5 shows that two variable parameters for the electron spin resonance condition are electromagnetic frequency, ν, and magnetic field, H. To gleam some insight about the defects in a solid, one of these parameters should be held constant while the other is varied. In EPR spectroscopy, a constant frequency electromagnetic field is applied to a sample, generating a standing wave. Simultaneously, a varying magnetic field is also applied. At the resonant condition described by equation 2.5, the standing wave is disturbed. The change in the standing wave is measurable, and this plot of reflected radiation versus magnetic field is referred to as the EPR spectrum [2].

Moreover, in a real system, the value of g is dependent upon a variety of factors. Studying the change in this value can provide some insight into the nature of a given system [7, 8]. Figure 2.2 from Ryan et al. illustrates EPR results in HfO_2 thin films compared to simulation [9]. Note that in this particular figure, the expected defect, a P_{b0} defect, is present, as well as an additional defect that was not found during the EPR simulation. The authors attribute the peak on the right to an oxygen vacancy in the HfO_2 film [9]. EPR therefore has the ability to illustrate which defects are present in solids provides meaningful information about the structure of a studied material.

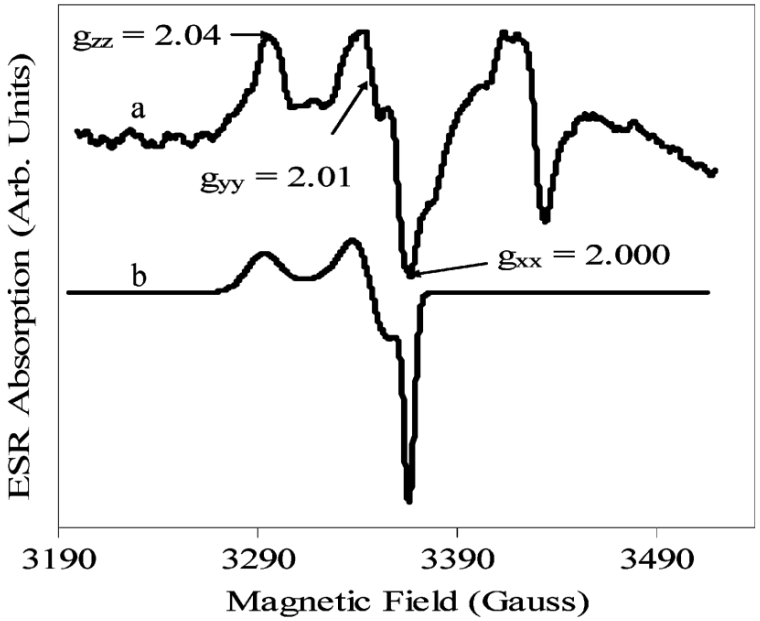

Figure 2.2: a) EPR trace of an HfO_2 film, and b) simulation of the same system. Figure from J. Ryan, P. Lenahan, A. Kang, J. Conley, G. Bersuker, and P. Lysaght, "Identification of the atomic scale defects involved in radiation damage in hfo/sub 2/based mos devices," IEEE transactions on nuclear science, vol. 52, no. 6, pp. 2272–2275, 2005.

2.2 Electrically Detected Magnetic Resonance

While EPR spectroscopy is an effective technique for studying defects present in material samples, it is less useful for nanoscale electronics [8]. For these devices, it is more appropriate to use electrically detected magnetic resonance (EDMR) spectroscopy [8, 10]. In EDMR, both a constant electromagnetic field and a varying magnetic field are applied, just like in EPR. However, instead of measuring the reflected portion of EM radiation, the spin-dependent current across the device is measured [11]. In doing so, information about the spin of carriers are considered [12]. EDMR therefore allows for the identification of electron transport mechanisms including recombination, scattering, and tunneling [4].

One advantage of EDMR spectroscopy is that it is about 10^7 times more sensitive than conventional EPR [13, 14]. Part of this increase in sensitivity stems from the nature of the investigation. Classic EPR spectroscopy considers all of the spin-active defects in a sample. By using current

or voltage instead of reflected radiation, only defects that impact the device performance are considered. The logistical drawback of this technique is that additional equipment is often need in addition to the spectrometer setup. This includes devices like preamplifiers and voltage sources, both of which are often needed to optimally bias the device and measure great enough current or voltage to see a signal amidst the noise.

EDMR has been used on a variety of systems. It has been used to assess the defects involved in negative bias temperature instabilities in 4H SiC MOSFETs [13]. In an atypical use case, it has been used on bulk SiC crystals [15]. It has been used to find deep silicon vacancies in SiC bipolar junction transistors and in SiC diodes [10, 14]. In emerging memory technology, EDMR has been used to study the switching mechanism of resistive random access memory and to describe the effect of radiation on these devices [8]. Moreover, in complex systems with featureless spectra, defect properties have been studied by varying the frequency of the applied electromagnetic field [16].

EDMR has been used to detect spin dependent recombination [11]. It is also an effective technique for identifying deep-level defects [10]. Relevant for this study, EDMR been used to detect spin-dependent trap-assisted tunneling (SDTAT) [11, 6, 8]. In SDTAT, electrons tunnel through traps in an oxide. From the Pauli exclusion principle, electrons with the same spin cannot occupy the same trap in the oxide. However, a magnetic field can be used to flip the spin of either an electron with energy to enter the trap or the electron in the trap. In doing so, the spins of the electrons differ, and thus the Pauli exclusion principle may be satisfied. This process is therefore spin dependent [11, 6, 8]. Figure 2.3 illustrates this process. SDTAT is important for this particular work because SDTAT is typically observed in oxides and describes the means by which an EDMR repsonse may be found as an electron tunnels through traps in an oxide [8]. Moreover, the major structural area of interest in the devices studied in this work are, generally, oxides [17, 18, 19, 20].

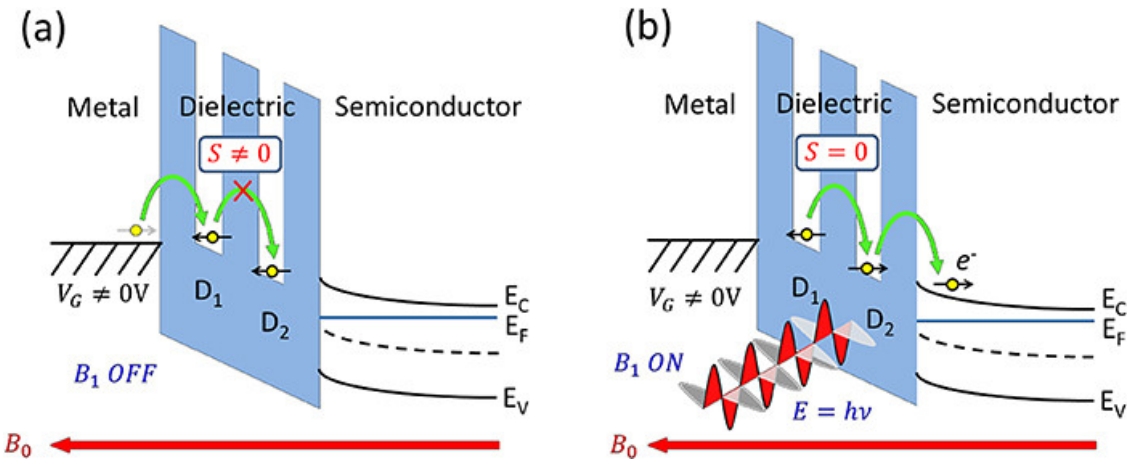

Figure 2.3: a) The triplet state, a forbidden transition; b) a singlet state, or allowed transition. An applied field can allow the spin to flip, changing the system from a triplet state to a single state and allowing for tunneling. In this case, the electron is tunneling through an oxide via SDTAT, with labels given to describe the system at a transistor gate. Figure from M. A. Anders, P. M. Lenahan, C. J. Cochrane, and J. van Tol, "Physical nature of electrically detected magnetic resonance through spin dependent trap assisted tunneling in insulators," Journal of Applied Physics, vol. 124, no. 21, p. 215105, 2018.

2.3 Near-Zero Field Magnetoresistance

2.3.1 Theory and Literature

Near-zero field magnetoresistance (NZFMR) is a relatively new technique that involves similar physics to conventional EPR and EDMR [3]. A change in magnetoresistance is detectable when preforming EDMR at low fields [21]. While conventional EPR and EDMR involve the flipping of a triplet state into a singlet state, NZFMR instead involves a mixing of states [6, 3, 22, 23]. This is because the mixed-state phenomenon occurs at low magnetic fields [22, 23].

It is speculated that the NZFMR response may be useful for determining information about the hyperfine interactions in electronics, in part because the mixed-state phenomenon often involves hyperfine interactions [3]. Moreover, NZFMR is, in practice, a DC measurement, and is believed to have substantial use in 3D integrated circuits; classic EPR and EDMR are both less applicable to these systems because of the dependency on high-frequency electromagnetic fields [3]. These

traits suggest that NZFMR has meaningful applicability in modern integrated circuit and device research.

While conventionally observable in EDMR, SDR has been demonstrated in the NZFMR as well. Cochrane and Lenahan demonstrate an approximately 1% change in current via $\Delta i/i$ measurement in a PN junction [4]. The authors report finding both an expected SDR response at low fields as well as an unexpected SDR response, dubbed the zero-field SDR response (ZFSDR), around $B = 0$ G. This response is visible on both traces included in figure 2.4. Moreover, a broadening of the SDR response was shown in the ZFSDR response, with a lower overall magnitude.

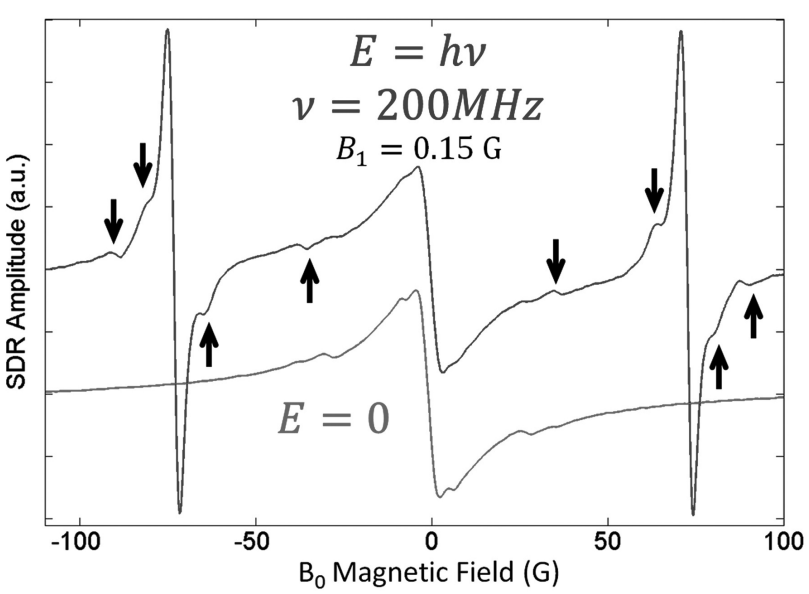

Figure 2.4: Low field and zero-field responses in a SiC diode. The top trace is with RF radiation applied, the bottom trace is without it. Adapted from C. J. Cochrane and P. M. Lenahan, "Zero-field detection of spin dependent recombination with direct observation of electron nuclear hyperfine interactions in the absence of an oscillating electromagnetic field," Journal of Applied Physics, vol. 112, no. 12, p. 123714, 2012. [Online]. Available: https://doi.org/10.1063/1.4770472

Also of note is a proof-of-concept paper by Ashton et al. In this paper, the researchers compare a variety of techniques on devices including planar MOSFETs, SiGe transistors, finFETs, SiO_2 oxides, and low-k dielectrics [3]. The work by Ashton et al. demonstrates that NZFMR can both be compared to EDMR, as well as possess potential for use in situations beyond conventional

EDMR. Specifically, the authors note that NZFMR should be a useful technique for analyzing 3D integrated circuits because it is not dependent on a applied field which is otherwise unable to penetrate a dense circuit. Moreover, it illustrates the need for further NZFMR spectroscopy studies.

2.3.2 Financial Considerations

If the NZFMR effect can be understood with the rigor and depth that currently exists for our understanding of EDMR, significant costs may be eliminated from resonance spectroscopy. EPR and EDMR require an oscillating electromagnetic field in order to meet the resonance condition outlined in equation 2.5. The specialized equipment needed for this system is a serious source of cost in resonance spectroscopy. NZFMR, however, does not require an applied electromagnetic field [4]. The elimination of these components from resonance spectroscopy may ultimately allow for systems be developed at a reduced cost.

Chapter 3

Resistive Random Access Memory

3.1 Resistive Random Access Memory Devices

Resistive random access memory (ReRAM) is an emerging and controversial memory. ReRAM is currently envisioned in literature as a viable candidate for future non-volatile memory [24, 18]. A ReRAM cell is typically built as a metal-insulator-metal stack with a metal oxide as in the insulator [17, 18, 19]. The metal oxide is typically a transition metal oxide; Hf and Ta are popular candidates [20]. This stack may be describes as a top electrode (TE), metal oxide, and bottom electrode (BE). Figure 3.1a illustrates a conventional ReRAM cell. Transition metal oxide ReRAM cells often include a metal cap between the TE and the transition metal oxide [20]. Figure 3.1b illustrates this structure.

Metal oxide ReRAM is believed to operate by means of forming, setting, and reseting a conductive filament within the metal oxide [19, 20, 24]. In bipolar ReRAM, a positive voltage is applied to a very high resistance, ”unformed” device. This application of relatively high voltage

is believed to cause the formation of a conductive filament in the metal oxide, thus ”forming” the device and leaving it in a low resistance state (LRS) [20]. Subsequently, a negative voltage may be used to break the CF, therefore ”resetting” the device to a high resistance state (HRS) [20]. A positive voltage, generally less than that needed for formation, may ”set” the device back into the LRS by reforming the CF. This alternation between the LRS and the HRS is how a device is switched back and forth between the ”on” and ”off” states. Many of these processes require the use of a compliance current to prevent damage to the device as the conductive filament forms [20]. Figure 3.2 illustrates a proposed model for the formation, set, and reset processes in an ReRAM device. Figure 3.3 illustrates IV data for the set and reset processes.

The switching mechanism in bipolar transition metal oxide ReRAM is a source of some interest and controversy in literature. It is believed that the CF in transition metal oxide ReRAM is made of oxygen vacancies [18, 20, 24, 25, 26]. When a positive voltage is applied to the TE, defects flood the oxide. When a negative voltage is applied, defects leave the oxide via diffusion. In subsequent SETs and RESETs, the oxygen vacancies are believed to move from the CF edge near the BE [18, 20, 24, 27, 28]. Moreover, the SET and RESET processes appear to be both field and temperature dependent [18].

This description of the switching mechanism, however, is rife with controversy. In some ReRAM models, oxygen vacancies are generate by the migration of oxygen atoms in the SET process and recombine during the RESET process [29, 30]. In others, however, it is believed that no vacancy generation and recombination occurs, and instead the vacancies remain present elsewhere in the cell before being SET again [31]. Moreover, both mechanisms are independently suggested to be present in bipolar switching, an inherently impossible conclusion.

3.2 EDMR on ReRAM

EDMR is, in theory, an excellent tool for identifying the nature of spin-active defects within resistive random access memory. However, EDMR on ReRAM only appears in literature once.

In "Total Ionizing Dose Effects on TiN/Ti/HfO_2/TiN Resistive Random Access Memory Studied via Electrically Detected Magnetic Resonance," McCrory et al. investigate hafnium oxide ReRAM [8]. While the authors report significant EDMR signals that are reportedly due to oxygen vacancies in ReRAM, they also report that only a small EDMR signal is present before radiation. Moreover, multiple doses of radiation in the devices seems to induce a negligible change in resistance. This suggests that while radiation induces spin-dependent electrically active defects in this author's sample of ReRAM, the devices are effectively radiation-hard, as noted by the negligible resistance change.

McCrory et al. report that the EDMR response is substantially bigger after increased radiation. These findings are clearly available in figure 3.4. By definition, the LRS in ReRAM has more current through a device than the HRS. McCrory et al., however, report that despite higher current, a higher current change is demonstrated in the HRS than in the LRS both before and after irradiation. These findings may suggest that a higher spin dependence is present in devices without a completely formed conductive pathway. Fittingly, it seems plausible that investigating the physical mechanism behind filament formation should help elucidate the nature of the defects potentially involved in ReRAM's operation. Investigating these types of devices and comparing resonance measurements at different points in the formation/reset/set process should therefore provide meaningful information to supplement and develop the findings both by McCrory et al. and other research groups.

Furthermore, low-field and zero-field resonance measurements have not appeared present in literature. It is possible that NZFMR measurements may provide further information about ReRAM that is currently not accounted for by EDMR or by other structural investigation techniques. Moreover, in conjunction with other projects comparing high-field and low-field measurements, the investigation of ReRAM with NZFMR may provide further information about how to best apply NZFMR and what information it can uniquely gleam about an electronic device.

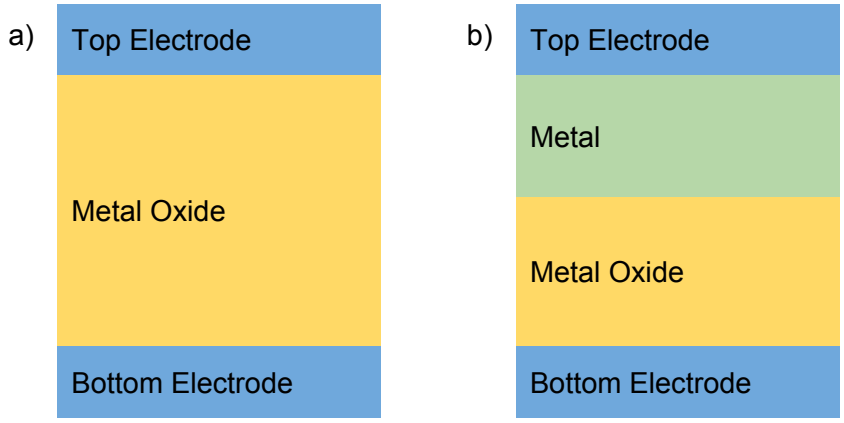

Figure 3.1: a) Typical ReRAM device structure; b) ReRAM device with metal cap.

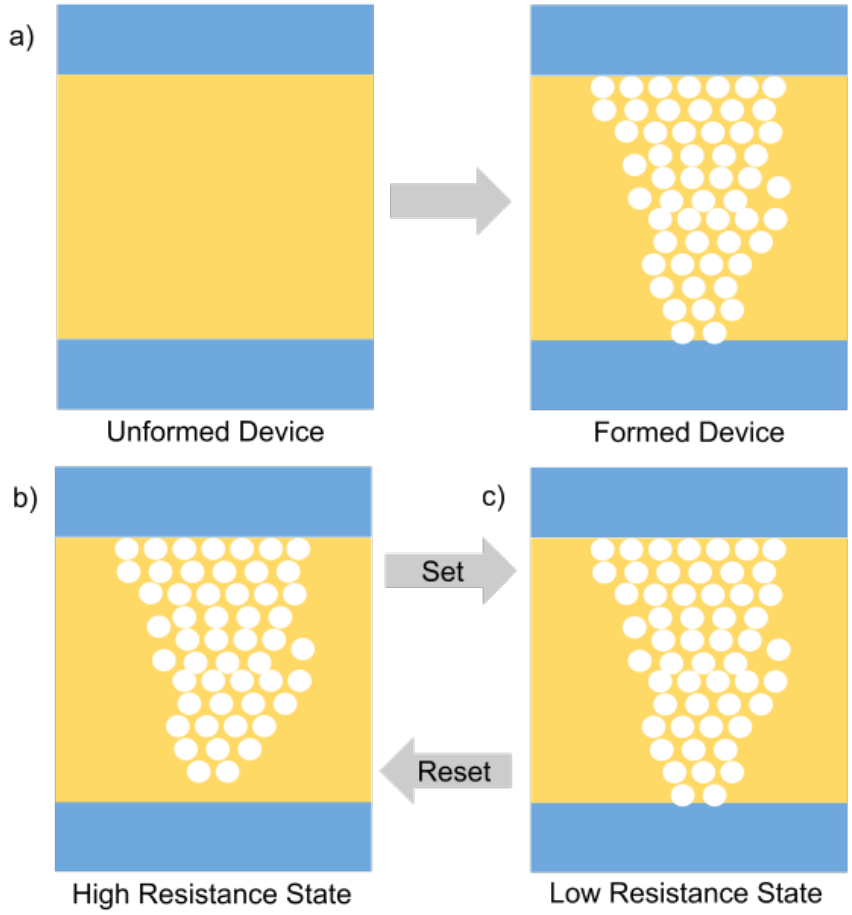

Figure 3.2: a) Formation of a conductive filament in a ReRAM device; b) ReRAM device after reset; c) ReRAM device after set process. Note that this is a proposed model, and variations exist.

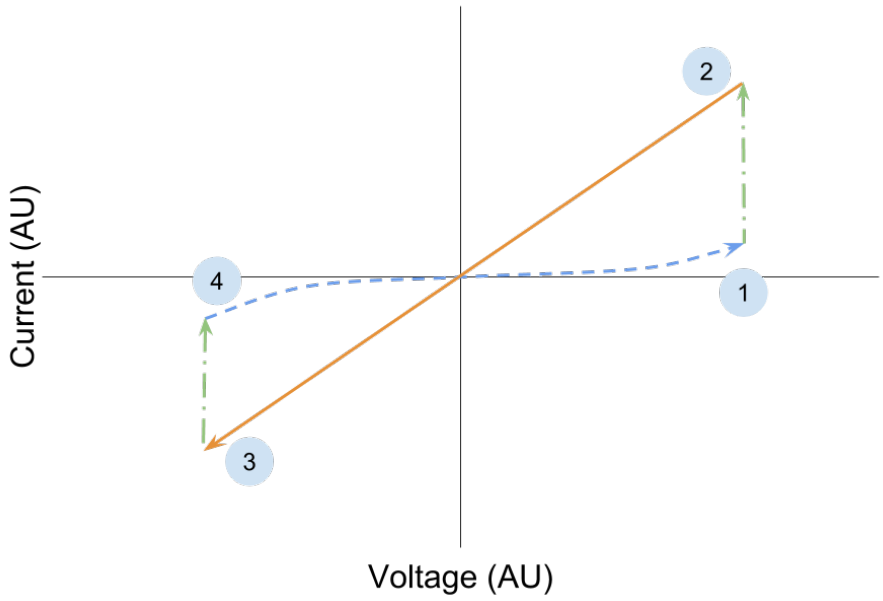

Figure 3.3: Typical ReRAM IV characteristics. The transition from 1 to 2 is the set process, and from 3 to 4 is reset. The orange, solid line is the ”on” state, and the dashed blue line is the ”off” state, with the dot-dashed line representing the transitions between states.

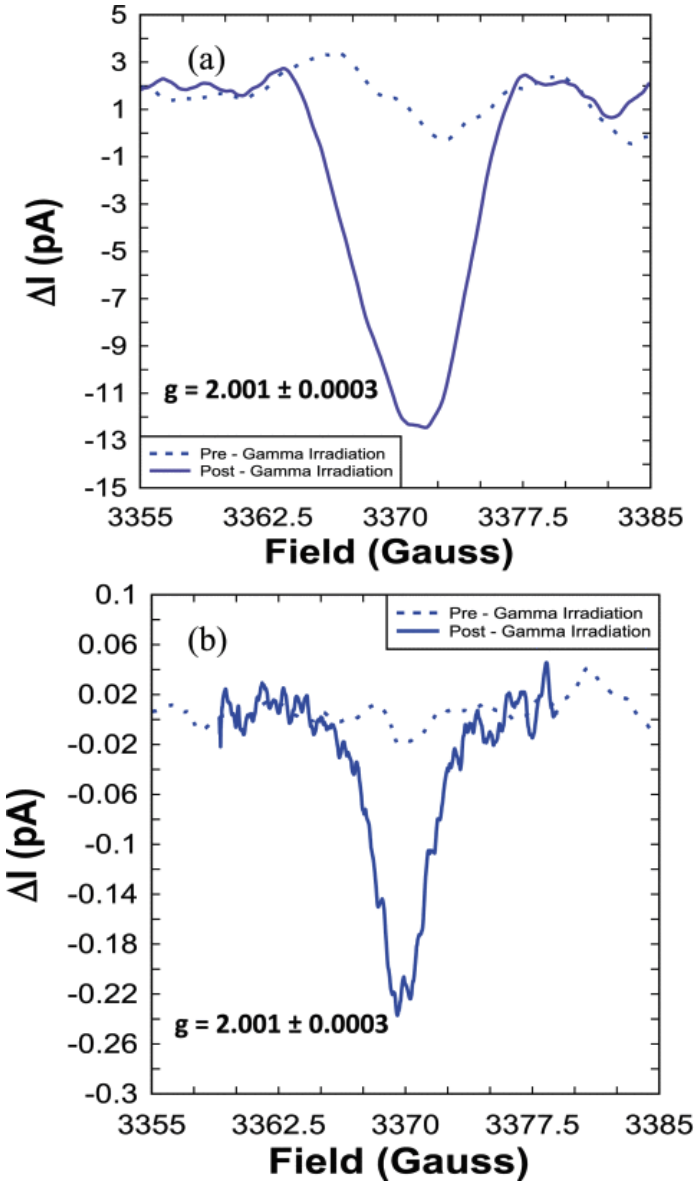

Figure 3.4: EDMR response in ReRAM in the LRS (top) and HRS (bottom), taken at .16 V and 5 V, respectively. Figure from D. J. Mccrory, P. M. Lenahan, D. M. Nminibapiel, D. Veksler, J. T. Ryan, and J. P. Campbell, "Total ionizing dose effects on tin/ti/hfo2/tin resistive random access memory studied via electrically detected magnetic resonance," IEEE Transactions on Nuclear Science, vol. 65, no. 5, pp. 1101–1107, 2018.

Chapter 4

Methods

4.1 Characterization

Samples of ReRAM from Sandia National Laboratories were acquired and processed for spectroscopy. The ReRAM samples were made with a 10 nm TaO oxide layer. The ReRAM arrays feature a crossbar architecture. Figure 4.1 illustrates the crossbar architecture used. In order to abide by the physical constraints of spectroscopy, the ReRAM cell chip was attatched to an insulting ”T.” The pads of a subject ReRAM cell were wire-bound to conductive strips on the T and to a USB port. Figure 4.2 illustrates a typical device processed for spectroscopy. ReRAM cells were then characterized for their initial resistances using a Hewlett Packard 4155A Semiconductor Parameter Analyzer. The semiconductor parameter analyzer was linked to a virtual instrument controller on a Lenovo computer running Windows 10 Enterprise.

4.2 Spectroscopy

Spectroscopy was carried out on a homemade spectrometer. The experimental setup uses a Stanford Research Systems Model SR570 Low-Noise Current Preamplifier, a Dell computer featuring Blue Spin Software, and a National Instruments USB X Series Multifunction Data Acquisition System (DAQ). A Hewlett Packard 8658B Signal Generator (.1-999MHz) set to a 72.2 MHz frequency applied a 17 dBm waveform. Figure 4.3 illustrates the device in the spectrometer. Figure 4.4 illustrates the network of devices used in the spectroscopy experiment. The EDMR and NZFMR response on an unformed ReRAM cell was measured using this system.

A 5 G modulation signal with a .5 time constant, scanning 80 G wide was used to identify a where the spectrum may occur on a partially formed device. A .01 V bias was applied, as preliminary testing indicated that the devices would form over time if left at higher voltage (approximately .05 V). This would overload the preamplifier circuit and would require a different sensitivity to be used. EDMR measurements often require many scans, typically more than 1000, in a device with consistent performance. This, combined with the dearth of quantitative models of ReRAM performance available, meant that it was necessary to use a low biasing condition of .01 V. Anecdotally, .02 V could be used in a completely unformed device, though a myriad of practical issues limit the ability to meaningfully report this finding thoroughly within this study and so it is only included as practical advice for future studies.

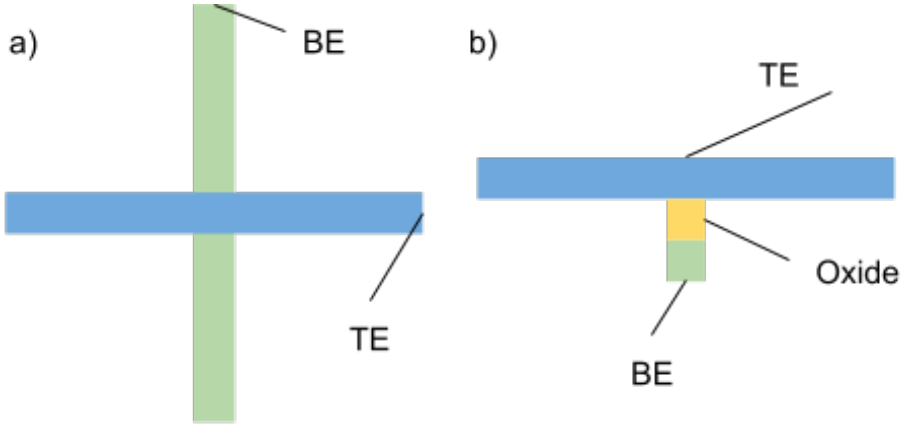

Figure 4.1: a) Crossbar structure from a top-down view; b) viewed from the side, such that the stack is visible.

Figure 4.2: Illustration of a typical device processed for spectroscopy, mounted to a T and connected to a USB port.

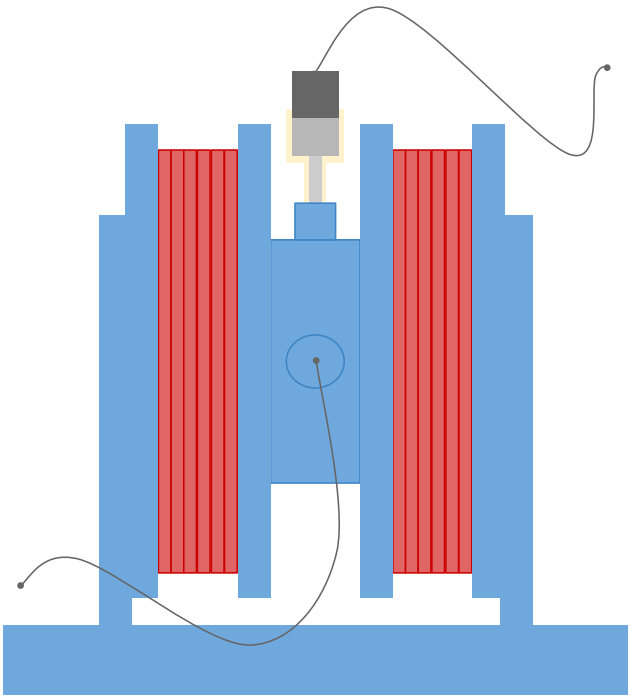

Figure 4.3: Illustration of device in lab-made spectrometer.

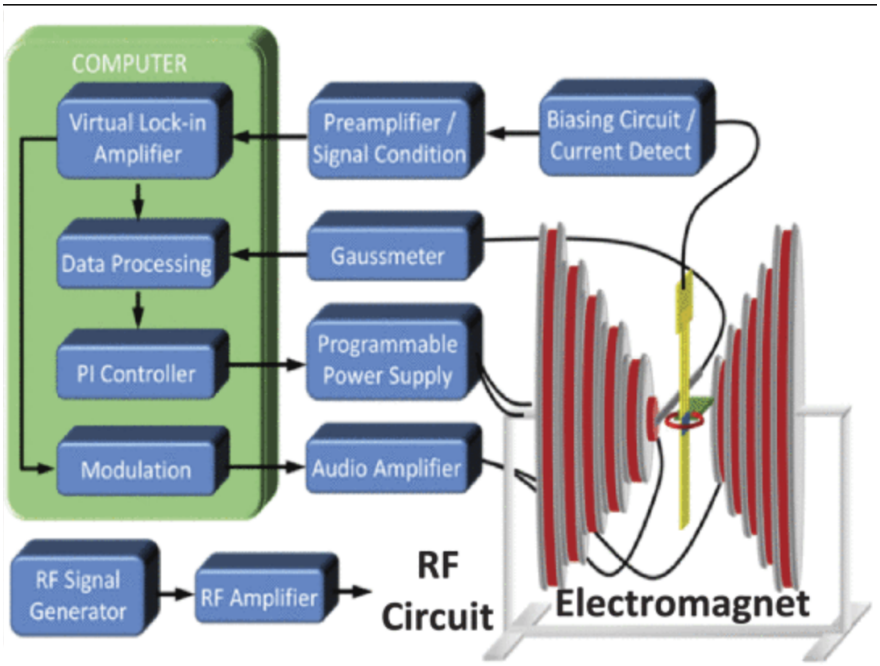

Figure 4.4: EDMR and NZFMR spectrometer system. Figure from J. P. Ashton, S. J. Moxim, P. M. Lenahan, C. G. Mckay, R. J. Waskiewicz, K. J. Myers, M. E. Flatte, N. J. Harmon, and C. D. Young, "A new analytical tool for the study of radiation effects in 3-d integrated circuits: Near-zero field magnetoresistance spectroscopy," IEEE Transactions on Nuclear Science, vol. 66, no. 1, pp. 428–436, 2019.

Chapter 5

Results

Figure ref? illustrates the performance of an unformed device from 0 V to switching. Note that a compliance current was used to limit potential damage to the device. Ultimately, this failure was too great and was impossible to switch into the HRS. Another device was partially formed (PFD) in preprocessing via electrostatic damage. This device was processed as it seemed plausible to contain relevant defects. Figure 5.2 illustrates the combination of device scans from 0 to .02 V and from 0 to -.02 V on the PFD. Overall, a device resistance of about 500 kΩ was measured.

Figure 5.3 shows early spectroscopic results of the PFD device. These results feature high asymmetry, and no notable resonance peaks. These results do, however, show a great NZFMR response.

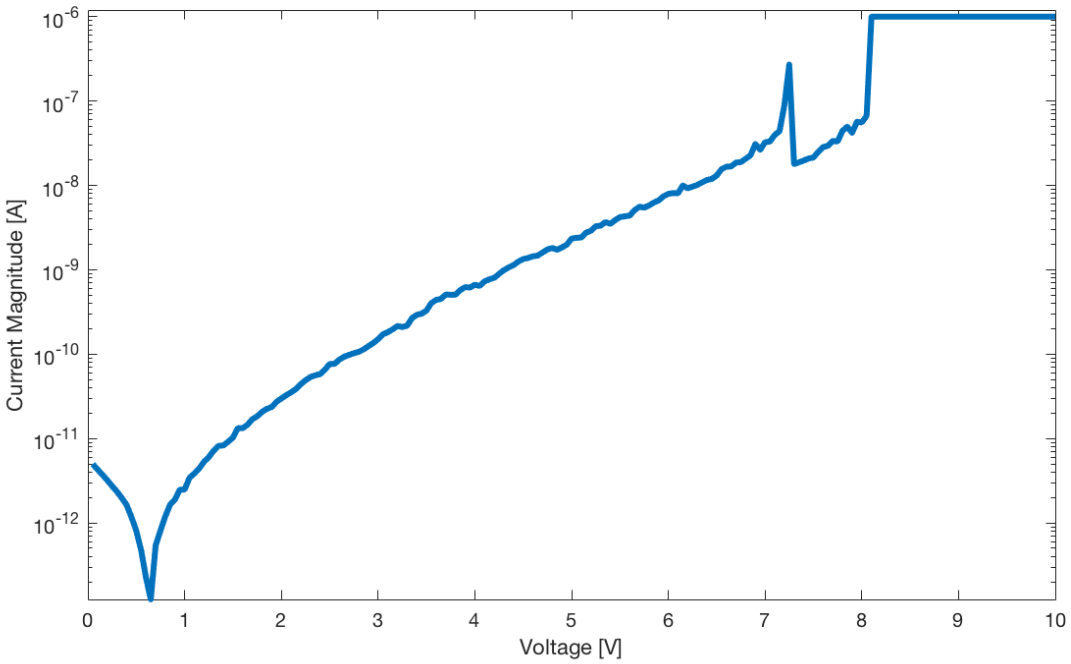

Figure 5.1: Formation of ReRAM device. Note that the current before the drop to 0 A was negative, and the current thereafter was positive in magnitude.

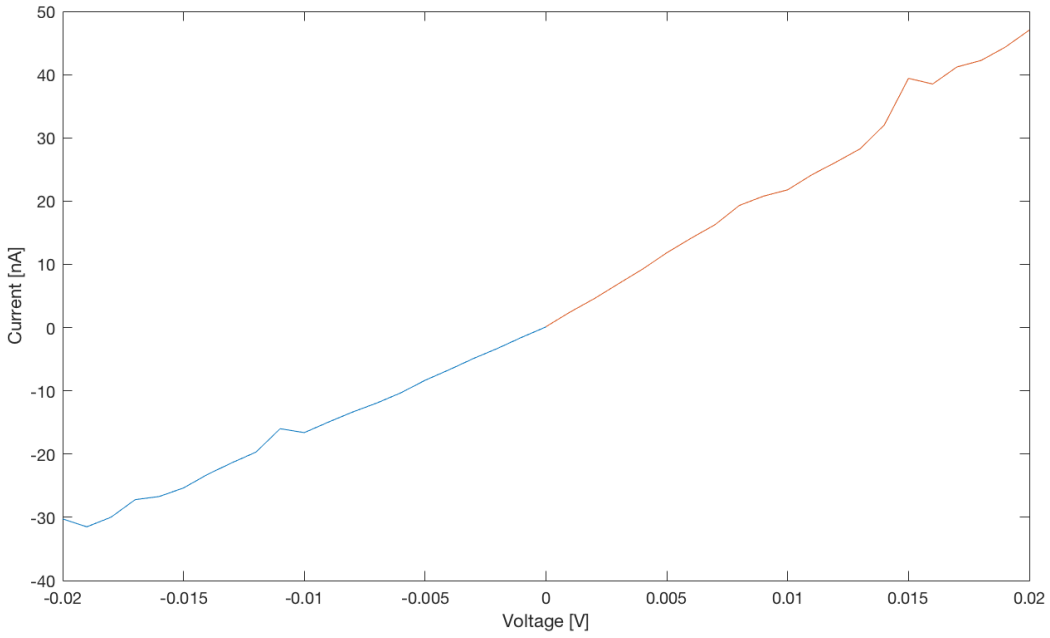

Figure 5.2: ReRAM device sampled from 0 V to .02 V and from 0 V to -.02 V.

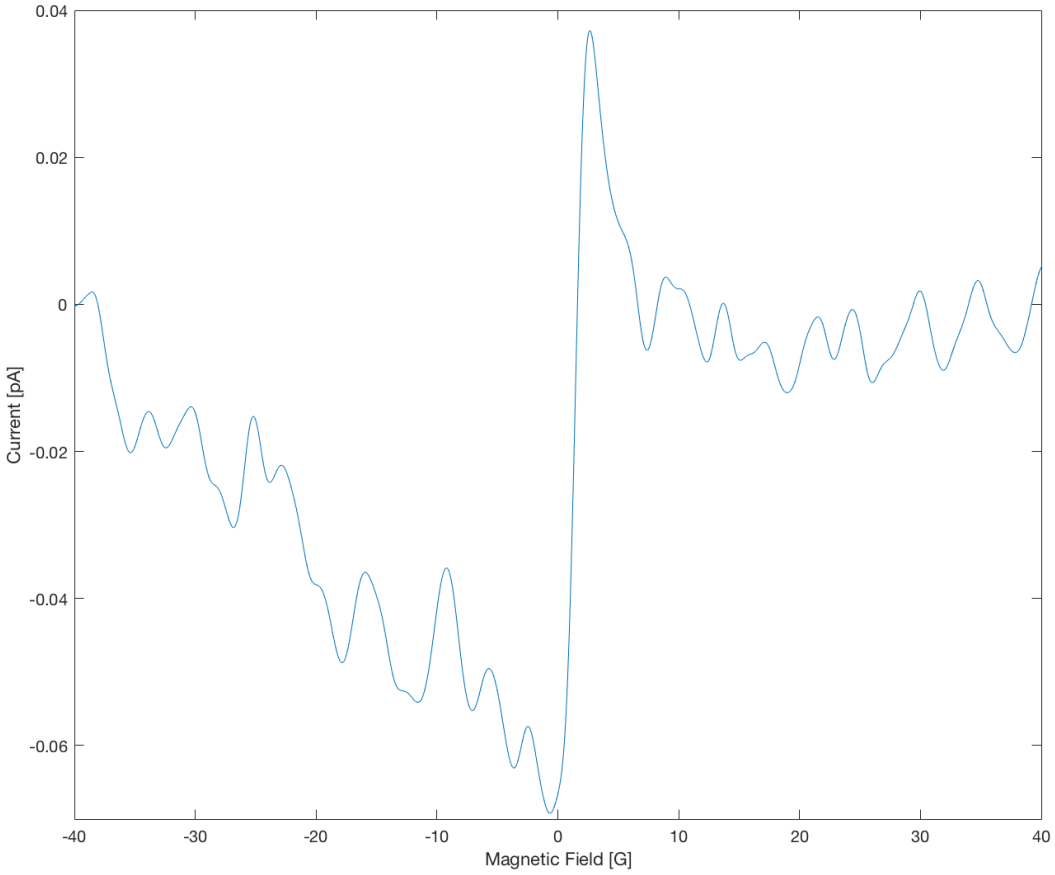

Figure 5.3: Resonance measurements of ReRAM. Note the large NZFMR signal, but almost lack of EDMR signals

Chapter 6

Discussion

6.1 Magnetic Resonance in Resistive Random Access Memory

Figure 5.1 shows the device potentially forming. It hit compliance current around just about 8 V. Of note is that the device experienced some form of soft-forming just before that. Additionally, the current until that point was demonstrated to increase linearly in the log scale. The implications of these findings are unclear and demand further investigation.

Figure 5.3 illustrates the results for low field and zero-field spectroscopy measurements on ReRAM. From the figure, it is clear to see a large zero-field signal, the NZFMR response. However, the EDMR response is equivalent or smaller than the magnitude of the noise given by this particular figure. The NZFMR response is not profoundly clear, despite being nontrivially larger than any present resonance signature, at least because of the noise present. Further analysis and fine-tuning is required to best isolate the NZFMR signal from any noise present and to most clearly show any detailed features in the system. For example, the presence of any nuclear hyperfine interactions are

unable to be interpreted from this signal due to the lack of clarity.

Still, the presence of a clear and unambiguous NZFMR response is, it itself, a useful finding. This finding supports the claim that an NZFMR response may be more readily present than an EDMR response, which may allow for quicker system scanning or more meaningful scanning in systems in which spin-dependent defects are not abundantly available for resonance measurements. The mixing of triplet and singlet states evidently may play a role in the NZFMR response of ReRAM that allows a higher current change in this system. These results do not provide substantial and useful information about the nature of ReRAM, but they do suggest that both NZFMR and general resonance measurements may have a meaningful role in studying the formation and switching mechanisms in ReRAM. Moreover, this study provides the first NZFMR response of ReRAM in any literature.

6.2 Future Work

This study is a small introduction into spectroscopic studies of ReRAM, and it primarily establishes that more work must be done to fully understand the forming and switching mechanisms of ReRAM at an atomic scale.

The findings illustrated in figure 5.1 may provide some information about the conduction mechanism in an unformed device. Future work should focus on mapping the device current to existing models of current, if only to elucidate potential means by which a spin dependence can be used. If the conduction mechanism is indeed tunneling, as is consistent with the SDTAT model, stability could perhaps be balanced against predicted current to uncover more information about the device via electron resonance.

First, it is pertinent that EDMR spectroscopy be done on these samples at x-band electromagnetic frequencies. While the EDMR response should be visible at low fields, low and zero-field resonance spectroscopy are still a relatively new techniques [4]. It would therefore be meaningful to compare low and high field EDMR responses. This information would help elucidate which

spin-dependent defects in ReRAM and would further develop the base of research available for interpreting resonance responses between different EM frequencies.

Second, it would be meaningful to compare responses at a range of temperatures. EDMR has been shown to have varying signal strength at different temperatures during internal, unpublished investigations of ReRAM. Given how small the resonance response is in the unformed ReRAM samples studied, even a small increase in signal size may allow for a clearer understanding of the structure of these devices.

Third, spectroscopic defect investigations should be done after irradiating these devices. In McCrory et al., the defect responses increase dramatically in magnitude, but do not appear to introduce different types of defects [8]. It seems sensible, then, that a similar method would add to the understanding of the defects in these devices.

6.3 Conclusion

In this study, low-field and zero-field measurements were made on TaO ReRAM. While limited results were found concerning resonance in the ReRAM studied, a clear an obvious NZFMR response was found. This response was unambiguous, but was not finely resolved. A variety of future studies were described, and the first foray into studying these devices with spectroscopy beyond McCrory et al. was made. A potential use of the NZFMR response was demonstrated in a system for which the NZFMR response is substation ally clearer than any EDMR response present. Furthermore, this study outlines the first NZFMR measurements in ReRAM.

Bibliography

[1] G. B. Silva, L. F. Santos, R. M. Faria, and C. F. O. Graeff, "Edmr of meh-ppv leds," *Physica B: Physics of Condensed Matter*, vol. 308, pp. 1078–1080, 2001.

[2] M. Brustolon and G. Giamello, *Electron paramagnetic resonance: a practitioner's toolkit*, 1st ed. Hoboken, N.J: Wiley, 2009.

[3] J. P. Ashton, S. J. Moxim, P. M. Lenahan, C. G. Mckay, R. J. Waskiewicz, K. J. Myers, M. E. Flatte, N. J. Harmon, and C. D. Young, "A new analytical tool for the study of radiation effects in 3-d integrated circuits: Near-zero field magnetoresistance spectroscopy," *IEEE Transactions on Nuclear Science*, vol. 66, no. 1, pp. 428–436, 2019.

[4] C. J. Cochrane and P. M. Lenahan, "Zero-field detection of spin dependent recombination with direct observation of electron nuclear hyperfine interactions in the absence of an oscillating electromagnetic field," *Journal of Applied Physics*, vol. 112, no. 12, p. 123714, 2012. [Online]. Available: https://doi.org/10.1063/1.4770472

[5] S. O. Kasap, *Principles of electronic materials and devices*, 3rd ed. Boston: McGraw-Hill, 2006.

[6] M. J. Mutch, P. M. Lenahan, and S. W. King, "Spin transport, magnetoresistance, and electrically detected magnetic resonance in amorphous hydrogenated silicon nitride," *Applied Physics Letters*, vol. 109, no. 6, p. 062403, 2016. [Online]. Available: https://doi.org/10.1063/1.4960810

[7] E. Frantz, "Zero-field magnetic resistance magnetometer and its applicability in deep space," Senior Thesis, The Pennsylvania State University, Old Main, State College, PA 16801, 2018, senior Thesis.

[8] D. J. Mccrory, P. M. Lenahan, D. M. Nminibapiel, D. Veksler, J. T. Ryan, and J. P. Campbell, "Total ionizing dose effects on tin/ti/hfo2/tin resistive random access memory studied via electrically detected magnetic resonance," *IEEE Transactions on Nuclear Science*, vol. 65, no. 5, pp. 1101–1107, 2018.

[9] J. Ryan, P. Lenahan, A. Kang, J. Conley, G. Bersuker, and P. Lysaght, "Identification of the atomic scale defects involved in radiation damage in hfo/sub 2/based mos devices," *IEEE transactions on nuclear science*, vol. 52, no. 6, pp. 2272–2275, 2005.

[10] G. Gruber, M. Koch, G. Pobegen, M. Nelhiebel, and P. Hadley, "An extended edmr setup for sic defect characterization," *Materials Science Forum*, vol. 740-742, pp. 365–368, 2013.

[11] M. A. Anders, P. M. Lenahan, C. J. Cochrane, and J. van Tol, "Physical nature of electrically detected magnetic resonance through spin dependent trap assisted tunneling in insulators," *Journal of Applied Physics*, vol. 124, no. 21, p. 215105, 2018.

[12] K. Fukuda and N. Asakawa, "Angular-dependent edmr linewidth for spin-dependent space-charge-limited conduction in a polycrystalline pentacene," *Frontiers in Materials*, vol. 4, 2017.

[13] P. Lenahan, M. Anders, R. Waskiewicz, and A. Lelis, "Bias temperature instabilities in 4h sic metal oxide semiconductor field effect transistors: Insight provided by electrically detected magnetic resonance," *Microelectronics Reliability*, vol. 81, pp. 1 – 6, 2018. [Online]. Available: http://www.sciencedirect.com/science/article/pii/S0026271417305681

[14] C. J. Cochrane, P. M. Lenahan, and A. J. Lelis, "Deep level defects which limit current gain in 4h sic bipolar junction transistors," *Applied Physics Letters*, vol. 90, no. 12, p. 123501, 2007. [Online]. Available: https://doi.org/10.1063/1.2714285

[15] T. Sato, H. Yokoyama, and H. Ohya, "Electrically detected magnetic resonance (edmr) measurements of bulk silicon carbide (sic) crystals," *Chemistry Letters*, vol. 35, no. 12, pp. 1428–1429, 2006.

[16] M. J. Mutch, P. M. Lenahan, and S. W. King, "Defect chemistry and electronic transport in low-k dielectrics studied with electrically detected magnetic resonance," *Journal of Applied Physics*, vol. 119, no. 9, p. 094102, 2016. [Online]. Available: https://doi.org/10.1063/1.4942675

[17] C. Mannequin, A. Delamoreanu, L. Latu-Romain, V. Jousseaume, H. Grampeix, S. David, C. Rabot, A. Zenasni, C. Vallee, and P. Gonon, "Graphene-hfo2-based resistive ram memories," *Microelectronic Engineering*, vol. 161, pp. 82 – 86, 2016. [Online]. Available: http://www.sciencedirect.com/science/article/pii/S0167931716302118

[18] A. Schönhals, R. Waser, and D. Wouters, "Improvement of set variability in taox based resistive ram devices," *Nanotechnology*, 2017.

[19] M. Aono and R. Waser, "Nanoionics-based resistive switching memories," *Nature Materials*, vol. 6, no. 11, pp. 833–840, 2007.

[20] D. Ielmini, "Resistive switching memories based on metal oxides: mechanisms, reliability and scaling," *Semiconductor Science and Technology*, vol. 31, no. 6, p. 63002, 2016.

[21] C. J. Cochrane, J. Blacksberg, P. M. Lenahan, and M. A. Anders, "Magnetic field sensing with atomic scale defects in sic devices," in *Silicon Carbide and Related Materials 2015*, ser. Materials Science Forum, vol. 858. Trans Tech Publications, 6 2016, pp. 265–268.

[22] N. J. Harmon and M. E. Flatté, "Spin-flip induced magnetoresistance in positionally disordered organic solids," *Physical review letters*, vol. 108, no. 18, p. 186602, 2012;2011;.

[23] N. J. Harmon and M. E. Flatté, "Semiclassical theory of magnetoresistance in positionally disordered organic semiconductors," *Phys. Rev. B*, vol. 85, p. 075204, Feb 2012. [Online]. Available: https://link.aps.org/doi/10.1103/PhysRevB.85.075204

[24] N. Sedghi, H. Li, I. Brunell, K. Dawson, Y. Guo, R. Potter, J. Gibbon, V. Dhanak, W. Zhang, J. Zhang *et al.*, "Enhanced switching stability in ta2o5 resistive ram by fluorine doping," *Applied Physics Letters*, vol. 111, no. 9, p. 092904, 2017.

[25] R. Waser, R. Dittmann, G. Staikov, and K. Szot, "Redox-based resistive switching memories – nanoionic mechanisms, prospects, and challenges," *Advanced Materials*, vol. 21, no. 25-26, pp. 2632–2663, 2009.

[26] A. Wedig, M. Luebben, D.-y. Cho, M. Moors, K. Skaja, V. Rana, T. Hasegawa, K. K. Adepalli, B. Yildiz, R. Waser, and I. Valov, "Nanoscale cation motion in taox, hfox and tiox memristive systems," *Nature Nanotechnology*, vol. 11, no. 1, p. 67, 2016.

[27] Y. Lu, B. Gao, Y. Fu, B. Chen, L. Liu, X. Liu, and J. Kang, "A simplified model for resistive switching of oxide-based resistive random access memory devices," *IEEE Electron Device Letters*, vol. 33, no. 3, pp. 306–308, March 2012.

[28] Y. Wang, Q. Liu, S. Long, W. Wang, Q. Wang, M. Zhang, S. Zhang, Y. Li, Q. Zuo, J. Yang, and M. Liu, "Investigation of resistive switching in cu-doped hfo2 thin film for multilevel non-volatile memory applications," *Nanotechnology*, vol. 21, no. 4, p. 045202, 2010.

[29] X. Guan, S. Yu, and H. . P. Wong, "On the switching parameter variation of metal-oxide rram—part i: Physical modeling and simulation methodology," *IEEE Transactions on Electron Devices*, vol. 59, no. 4, pp. 1172–1182, April 2012.

[30] D.-h. Kwon, K. M. Kim, J. H. Jang, J. M. Jeon, M. H. Lee, G. H. Kim, X.-s. Li, G.-s. Park, B. Lee, S. Han, M. Kim, and C. S. Hwang, "Atomic structure of conducting nanofilaments in tio2 resistive switching memory," *Nature Nanotechnology*, vol. 5, no. 2, pp. 148–53, 02 2010, copyright - Copyright Nature Publishing Group Feb 2010; Last updated - 2014-03-24. [Online]. Available: http://ezaccess.libraries.psu.edu/login?url=https://search-proquest-com.ezaccess.libraries.psu.edu/docview/868642355?accountid=13158

[31] S. Larentis, F. Nardi, S. Balatti, D. C. Gilmer, and D. Ielmini, "Resistive switching by voltage-driven ion migration in bipolar rram—part ii: Modeling," *IEEE Transactions on Electron Devices*, vol. 59, no. 9, pp. 2468–2475, Sep. 2012.

William Barker

Education

2015–2019 **Bachelor of Science in Engineering Science**, *The Pennsylvania State University*, University Park, PA.

Dual Honors from Schreyer Honors College and the College of Engineering

Experience

2018–Present **Researcher**, *The Pennsylvania State University*, University Park, PA.

- Developed new electron resonance spectroscopy techniques including near-zero field magnetoresistance;
- Analyzed defects in nanoelectronic devices including resistive random access memory and silicon MOSFETs;

2018–Present **Teaching Intern**, *The Pennsylvania State University*, University Park, PA.

- Instructed during recitations for several hundred undergraduate Statics and Strength of Materials students;
- Enhanced instructional aid by preliminarily assessing content and hosting office hours weekly;

2015–2017 **Researcher**, *The Pennsylvania State University*, Abington, PA.

- Assessed the effectiveness of mathematical stability indices in predicting falls during human gait;
- Prototyped musculoskeletal model featuring neural controls and open-source software;

2015–2015 **Intern**, *Eli Lilly and Company*, Warminster, PA.

- Designed a multimedia platform to engage and support clinical trial community;
- Piloted a program that now offers innovative think-tank internships to dozens of students annually;

Presentations

SIAMOC Barker, W., & Talaty, M. (2016, Oct) *Clarification of Floquet Multipliers and State Space Reconstruction in Bipedal Gait Stability – A Computer Simulation Study*. Poster session presented at The Italian Society of Clinical Movement Analysis in Milan, Lombardy, Italy.

MC REU Barker, W., Talaty, M., & Moore, J. (2016, July) *Expansion of an Existing Neuromusculoskeletal Human Gait Model to OpenSim*. Presented at The Pennsylvania State University Multi Campus Research Experience for Undergraduates Research Symposium in University Park, PA, USA.

Medicine X Barker, W., Izak M., & Romanyszyn, J. (2015, Sept) *Art Inspiring Action in Clinical Research*. Talk presented at Stanford Medicine X in Stanford, CA, USA.

Technical Skills

Spectroscopy Electrically Detected Magnetic Resonance, Electron Paramagnetic Resonance

Software MATLAB, Python, C++, Molecular Workbench, LaTeX, Microsoft Office

Activities

2018–present **President**, *Society of Engineering Science*.

2017–2018 **Student Facilities Chair**, *Society of Engineering Science*.

2018–present **Student Member**, *Institute of Electrical and Electronics Engineers*.

Awards

Student Marshal for Engineering Science, Class of 2019

Frasier Merit Award in Engineering Science and Mechanics

Winner of Eli Lilly Incubator Challenge

Dean's List, Fall 2015 - Spring 2018

The President's Freshman Award